Cellulose (2024) 31:6517–6533
https://doi.org/10.1007/s10570-024-05979-6

ORIGINAL RESEARCH

Functionalization of cotton fabrics through PEI/PA/FeAl ternary system with enhanced flame retardance and antibacterial properties

Qingyi Li · Yakun Zong · Yuanzhang Jiang · Jun Zhang · Ruifang Zhao · Jianming Chen · Yidong Shi · Lin Tan

Received: 9 March 2024 / Accepted: 23 May 2024 / Published online: 30 May 2024

Abstract Cotton fabrics are widely used in clothing, packaging, and medical applications because of their excellent comfort, breathability, and low cost. However, it poses a threat to use them in specific scenarios, where flame retardance and antibacterial activity are highly desired. In this work, we propose the functionalization route by using layer-by-layer assembly of polyethyleneimine (PEI), phytic acid (PA), iron (Fe^{3+}), and aluminum (Al^{3+}) ions on cotton fabrics. Interestingly, the modified cotton fabric showed good biocompatibility in the cell viability (> 70%) and hemolysis (< 3%) test. In addition to biocompatibility, the antibacterial performance was largely improved for the modified cotton fabric with the antibacterial efficacy of > 99% due to the presence of Fe^{3+} and Al^{3+} that work in a synergistic manner. In term of flame retardance, the modified cotton fabric exhibited self-extinguishing characteristics in vertical burning experiments, with the Limiting Oxygen Index (LOI) of 35.0%. The excellent flame-retardant property was further supported by the results in cone calorimetry test, thermal gravimetric analysis, and TG-IR test, elucidating the underlying mechanism that rapid formation of dense char layer by the thermal decomposition of PEI/PA/FeAl system is effective to prevent the spreading of flame and thus protect the cotton from burning. This work provides a strategy to achieve multifunctionality on cotton fabrics, which may inspire the design on other types of fabrics or materials for extended applications.

Keywords Multifunctional cotton fabrics · Flame retardant · Antibacterial · Cytocompatible

Supplementary Information The online version contains supplementary material available at https://doi.org/10.1007/s10570-024-05979-6.

Q. Li · Y. Zong · Y. Jiang · Y. Shi · L. Tan (✉)
College of Biomass Science and Engineering, Key Laboratory of Biomass Fibers for Medical Care in Textile Industry, State Key Laboratory of Polymer Materials Engineering, Sichuan University, Chengdu 610065, China
e-mail: tanlinou@scu.edu.cn

Q. Li · Y. Zong · Y. Jiang · Y. Shi · L. Tan
Yibin Institute of Industrial Technology/Sichuan University, Yibin Park, Yibin 64460, China

J. Zhang · J. Chen (✉)
Research Institute for Intelligent Wearable Systems and Research Centre of Textiles for Future Fashion, School of Fashion and Textiles, The Hong Kong Polytechnic University, Kowloon, Hong Kong 999077, China
e-mail: jianming.chen@polyu.edu.hk

R. Zhao
Sichuan Province Fiber Inspection Bureau, Chengdu 610010, China

Introduction

Cotton, one of the most abundant natural fibers, can be easily processed into fabrics for various applications, such as apparel, furniture, automotive

upholstery, and healthcare due to their good biodegradability, water absorption, breathability, skin-friendliness, and comfort, (Lambert et al. 2019). However, the flammability, as the Achilles heel of cotton fabrics, largely limits their applications in other fields (Li et al. 2021). Therefore, it is of great significance and interest to explore effective and green methods to improve the flame retardance of cotton fabrics with minimum intervention on their original properties.

Halogenated flame retardants have been intensively applied on cotton fabrics mainly because of their high flame-retardant efficiency with low content required. However, the decomposed products from halogen-containing flame retardants are usually toxic and bioaccumulative (Page et al. 2023), and thus this type of flame retardant has been banned in many countries since 2003 (Özer and Gaan 2022). With increasing attention on the ecosystem, various halogen-free flame retardants rich in nitrogen and phosphorus elements have been developed as environmentally friendly flame retardants (Horrocks 2011). As N-P flame retardants, Proban® CC (tetrakis (hydroxymethyl) phosphonium salt) and Pyrovatex® CP (N-hydroxymethyl-3-(dimethoxy-phosphine acyl) propionamide) (Yang et al. 2005; Horrocks 2011) are two commercially products for cotton fabrics with exhibiting excellent flame retardance and durability, but formaldehyde is inevitably released during production and application (Lazar et al. 2020), which is hazardous to the environment. It was reported that once the N-P flame retardant system was further combined with other functional groups or elements, the flame retardance of cotton fabrics could be enhanced through the synergistic interaction between flame-retardant elements (Kappes et al. 2016; Xu et al. 2019; Sun et al. 2021; Chen et al. 2021; Rao et al. 2021; Li et al. 2023; Ding et al. 2023).

Of various intumescent flame retardants (IFR), the composite flame retardant containing nitrogen and phosphorus elements is favorably adopted with the merits in low smoke and toxicity but high efficiency. (Osimitz et al. 2019). IFR functions to form a charcoal layer that protects the substrate from flames after a series of chemical reactions along with the combustion. Biomass-derived phytic acid (PA) is a non-toxic, sustainable, and environmentally friendly natural substance extracted from legumes and grains, consisting of six phosphate groups. When PA is applied to cotton fabric, it could induce the degradation of cellulose below 300 ℃, catalyze dehydration reactions, and facilitate carbonization during combustion (Chen et al. 2015). Hence, a protective layer can be rapidly formed on the fabric treated by PA before the orderly decomposition of the fabric (Sykam et al. 2021). However, it risks to degrade the cellulose solely using PA as the flame-retardant component and interestingly this issue can be well addressed by combining itself with amine-functionalized molecules or polymers (Barbalini et al. 2020; Sykam et al. 2021) in an IFR system. The negative charges enable the PA to closely bind with amine compounds (such as polyethyleneimine, PEI) carrying positive charges through electrostatic interaction to form flame retardants of the P-N system (Fang et al. 2019, 2020; Ye et al. 2021). PEI, polycations with abundant amine groups, are capable of interacting with polyanions to form the flame-retardant complex system. The PA and PEI system was reported by Cheng et al. (2019) as a polyelectrolyte complex, which was prepared at pH 1.5 and added onto the surface of wool fabric with an insoluble flame-retardant coating layer formed. Compared to the LBL (layer by layer) assembly, this coating process is more streamlined to exhibit stable flame-retardant properties on wool fabrics. As recently summarized by Holder et al. (2017), flame-retardant nanocoatings can be prepared by LBL deposition of positively charged PEI and negatively charged components, like poly phosphonium, phosphate graphene oxide, montmorillonite clay, and silica nanoparticles, to enhance the flame retardance of cotton, polyester, and cotton/polyester blended fabrics by suppressing the heat and smoke released from fabrics. Aluminum and iron are classified as flame-retardant elements and can be directly applied onto the surface of cotton fabrics. But their fair flame retardance and low washability make them hardly utilized independently as flame retardants. Interestingly, it was found that aluminum ions could synergize with phosphorus and nitrogen elements, demonstrating better flame retardant performance on cotton fabrics than those without aluminum ions. (Hao et al. 2019) Moreover, the whiteness of fabrics was improved by the addition of aluminum ions. It remains unclear to investigate the role and function of iron or iron/aluminum ions in the IFR system.

In this work, we incorporate Fe/Al ions with PEI and PA through LBL assembly on cotton fabrics with multifunctionalities. In this PEI/PA/FeAl ternary

system, PEI and PA work to serve as the main IFR, which shows enhanced flame retardance by the aid of metallic ions, i.e., Fe/Al ions. It is worth noting that the metallic ions can be tightly immobilized through the chelation by coordinating with PA, suggesting good washability and durability for functional cotton fabrics. Intriguingly, not only can the metallic ions functions as the flame-retardant elements, but also plays a role on the antibacterial property. Overall, the cotton fabrics modified with PEI/PA/FeAl show excellent biocompatibility, antibacterial activity, and flame retardance. The strategy and results obtained in this work provide valuable insights into the design of environmentally friendly multifunctional cotton fabrics for broad applications.

Experimental section

Materials

Sodium hydroxide, ferric sulfate hexahydrate, and aluminum sulfate octa decahydrate were supplied by Chengdu Kelong Chemical Industrial Reagent Co. (Chengdu, China). Polyethyleneimine (PEI, $M_w = 10{,}000$, 99%) was purchased from Aladdin Chemistry Co. Ltd. (Shanghai, China). Phytic acid (PA, 70 wt% in water) was purchased from Shanghai Titan Technology Co. Ltd. Anhydrous ethanol was purchased from Chengdu Jinshan Chemical Reagent Co. Ltd. Cotton fabrics were provided by the Functional Fiber Laboratory of Sichuan University. *Escherichia coli* (ATCC8739) and *Staphylococcus aureus* (ATCC6538) were purchased from Shanghai Luwei Technology Co. Ltd.

LBL assembly of PEI/PA/Fe/Al on cotton fabrics

Cotton fabrics were pretreated using 4 wt% sodium hydroxide solution at 80 °C for 1 h, then rinsed thoroughly with deionized water, and finally dried in the oven. The pretreated cotton fabrics (10×10 cm^2) were immersed in 50 mL of PEI solution (2 wt%) for 1 h and dried. Subsequently, the PEI-coated fabrics were transferred to 50 mL of PA solution (2 wt%) for another 1 h. Then, the PA-PEI-coated fabrics were immersed in 50 mL of 1 wt% $Fe_2(SO_4)_3 \cdot 6H_2O$ solution for 1 h. The treated fabrics were rinsed using deionized water for 30 s and dried. The LBL assembly was repeated twice and the treated samples were labeled as Cotton-PEI/PA/Fe. Similarly, Cotton-PEI/PA/Al can be prepared by replacing the $Fe_2(SO_4)_3 \cdot 6H_2O$ with $Al_2(SO_4)_3 \cdot 18H_2O$. As expected, both 1 wt% $Fe_2(SO_4)_3 \cdot 6H_2O$ and 1 wt% $Al_2(SO_4)_3 \cdot 18H_2O$ were taken in the third step of coating treatment to prepare the sample of Cotton-PEI/PA/FeAl.

Characterization

The functional groups of samples were investigated by attenuated total reflection Fourier transform infrared spectroscopy (ATR-FTIR, Tracer-100, Japan) in the range of 650–4000 cm^{-1}, with 32 scans at 4 cm^{-1} resolution. An X-ray photoelectron spectrometer (XPS, Shimadzu Kratas AXIS SUPRA, Japan) was used to analyze the elemental compositions on the surface of samples. Scanning electron microscope (SEM, SU3500, Hitachi, Japan) was used to observe the morphology of samples; all samples were coated with Au before measurement. Energy dispersive spectroscopy (EDS, IE 3000, UK) was used to map the distribution of various elements on the sample surface. The water contact angle can be analyzed by the contact angle tester (WCA, HKCA-40, HAKO, Beijing, China). The water vapor transmission rate (WVTR) of the coated fabrics was calculated by recording the water loss in the cotton fabrics at 38 ℃ with RH of 50% according to the standard of GB/T 12704.2–2009:

$$WVTR\left(mg \bullet cm^{-2} \bullet h^{-1}\right) = \frac{M_0}{S \times H} \times 100\% \quad (1)$$

where M_0 is the mass of water loss (mg) during the specified time, S represents the area (cm^2) of the bottle mouth, and H denotes the evaporation time (h).

The water absorption of cotton fabrics was tested according to the static immersion test reported in the improved ATCC Technical Manual 2001. To be specific, 1 g of dry sample (mass M_0) was immersed in a beaker containing 200 mL of water. 12 h later, the sample was removed and suspended vertically until no water dripped for 30 s. The sample was weighed as M_1. Three parallel samples were taken in each group. The formula for calculating water absorption was as follows:

$$K(\%) = \left(\frac{M_1 - M_0}{M_0}\right) \times 100\% \quad (2)$$

The mechanical properties of the samples were assessed through tensile measurements using an Electronic universal testing machine (EUT4104, China), in accordance with the standard method GB/T 3923.1–2013. The tensile speed was set at 20 mm/min, and each sample was subjected to tensile testing at a gauge length of 200 mm, with 10 repeats per sample, including 5 repeats for warp yarns and another 5 repeats for weft yarns.

The whiteness of the fabric surface was measured by a colorimeter CM3700A (Konica Minolta Inc., Japan). The cytotoxicity of samples was performed by using the mouse skeletal muscle L929 cell and cell counting kit-8 (CCK-8) according to the GB/T16886.5–2003 standard (Liu et al. 2020; Wu et al. 2021). Briefly, the L929 cells were stored in 96-well plates at a density of 2×10^3 cells per well in DMEM containing 10% FBS and 1% penicillin–streptomycin and cultured in a 37 °C, 5% humidified CO_2 incubator. The fabric samples were sterilized on both sides by UV irradiation, and then continuously macerated and stirred in DMEM medium at 37 ℃ for 24 h to obtain the extracts. After that, the corresponding extract was used to replace the preserved L929 cell culture medium. After incubation for 24 h, CCK-8 reagent was added and mixed to incubate for 2 h, and then the absorbance was detected by enzyme labeling instrument (Varioskan, Thermo Fisher Scientific). The cell viability was calculated as follows:

$$cellular\ activity(\%) = \frac{A_W - A_B}{A_N - A_B} \times 100\% \quad (3)$$

where, A_W, A_N, and A_B are the absorbance at 450 nm for the sample, negative control, and blank control.

Fresh rabbit blood was diluted with PBS buffer (pH 7.4) and centrifuged at 3500 rpm for 10 min, and the supernatant was removed to isolate the hemoglobin cells. The above steps were repeated 3 times until the supernatant was clear. Subsequently, the washed erythrocytes were added to PBS buffer to make erythrocyte suspension with a final concentration of 10% (v/v). Then, the sample of Cotton, Cotton-PEI/PA/Al, Cotton-PEI/PA/Fe, and Cotton-PEI/PA/FeAl (1×1 cm^2) were each placed into 1 mL centrifuge tubes containing 1 mL of erythrocyte suspensions and incubated for 2 h at 37 ℃. For comparison, the erythrocyte suspension diluted with PBS and ultrapure water was used as negative and positive control, respectively. Finally, the erythrocyte suspension after 2 h of incubation was centrifuged again at 3500 rpm for 10 min, the supernatant was collected and the absorbance at 540 nm was measured by UV–visible spectrophotometer to determine the release of hemoglobin, with 5 parallel samples used in each group. The hemolysis rate of the material was calculated using the formula:

$$hemolysis(\%) = \frac{OD_{sample} - OD_{negative\ control}}{OD_{positive\ control} - OD_{negative\ control}} \times 100\% \quad (4)$$

Where OD_{sample} is the absorbance of the experimental group, $OD_{positive\ control}$ is the absorbance of the positive control group and $OD_{negative\ control}$ is the absorbance of the negative control group.

The antibacterial performance of samples was evaluated according to the GB/T 20944.2–2007 and the GB/T 20944.1–2007 method. The bacterial morphology was observed by SEM. Fabric toxicity to bacteria was assessed by visual fluorescence imaging and bacterial cell viability was determined by Syto 9 and propidium iodide (PI) dye (Invitrogen Detection Technologies, USA) by confocal laser scanning microscope (Leica Microsystems CMS GmbH STELLARIS 5, Germany). In order to check the synergistic antibacterial activity of associated iron ion and aluminum ion combinations, the Fractional Inhibitory Concentration (FIC) index was studied against *S. aureus* and *E. coli*, Minimum Inhibitory Concentration (MIC) was first determined by plate spreading method. The FIC index determination was carried out via a checkerboard method (Hemaiswarya et al. 2008), and the fractional inhibitory concentration (FIC) index was calculated using the formula $FIC = MIC_{(Fe-Al)}/MIC_{Fe} + MIC_{(Fe-Al)}/MIC_{Al}$. The FIC index ≤ 0.5 indicates synergism effect, while that ≤ 0.5 to ≥ 1, 1 to 4 or > 4 mean additive, irrelevant or antagonism effects.

Thermogravimetric analysis was performed using a TGA8000 Thermogravimetric Analyzer (PerkinElmer, USA) under nitrogen and oxygen atmospheres with a ramp rate of 10 °C/min and a temperature range of 40—750 °C. CZF-5 horizontal vertical combustion tester (Beijing Aerospace Zongheng Inspection Instrument Co., Ltd.) was used to

carry out vertical combustion experiments on the samples (300×70 mm^2) according to the standard method of GB/T 5455–2014, and the samples were ignited with a vertical flame for 12 s. The sample (100×100 mm^2) was subjected to cone calorimetry (CCT) using i-CONE type cone calorimeter (FT Technologies, USA) according to the ISO5660-1 standard with the heat flow density of 50 kW/m^2. The Limiting Oxygen Index (LOI) test was carried out on the sample (150×56 mm^2) by using a JF-3 limiting oxygen index tester (Nanjing Jiangning District Analytical Instrument Factory, China) according to GB/T 5454–1997 standard.

The LOI of prepared fabrics was examined after being exposed to UV light for 1, 3, 5, and 7 days, respectively, and their flame retardant resistance to washing and soaping was conducted according to the standard FZ/T 73023–2006. Initially, 3 L of deionized water were poured into the washing machine, followed by adding the flame retardancy fabric (10 g) and an accompanying washing fabric (90 g), either polyester or polyester-cotton. Each washing cycle lasted for 5 min, and the whole washing process was repeated after 30 cycles. The soaping procedure was similar to the above process except for the addition of 0.6 g detergent during washing. Upon completing the final cycle of the soaping experiment, it was essential to utilize a substantial amount of deionized water to completely eliminate any residual detergent on the fabric, followed by dehydration and drying. Finally, the LOI of the fabrics was determined. Thermogravimetric-IR spectra (TG-IR) of the samples were obtained by using a Clarus SQ 8 T thermogravimetric-IR coupler (PerkinElmer, USA) under a nitrogen atmosphere at 40–700 ℃ with a heating rate of 50 ℃/min. All the above measurements were repeated at least three times to obtain the mean and standard deviation, except as specified in the standard.

Results and discussion

Characterization of surface structure of functional cotton fabrics

The modified functional cotton fabrics were prepared through LBL assembly as shown in Fig. 1. PEI, PA and metallic ions were introduced onto the fabric in a specific order. This rational design is made according to individual functions and roles. PEI was first coated

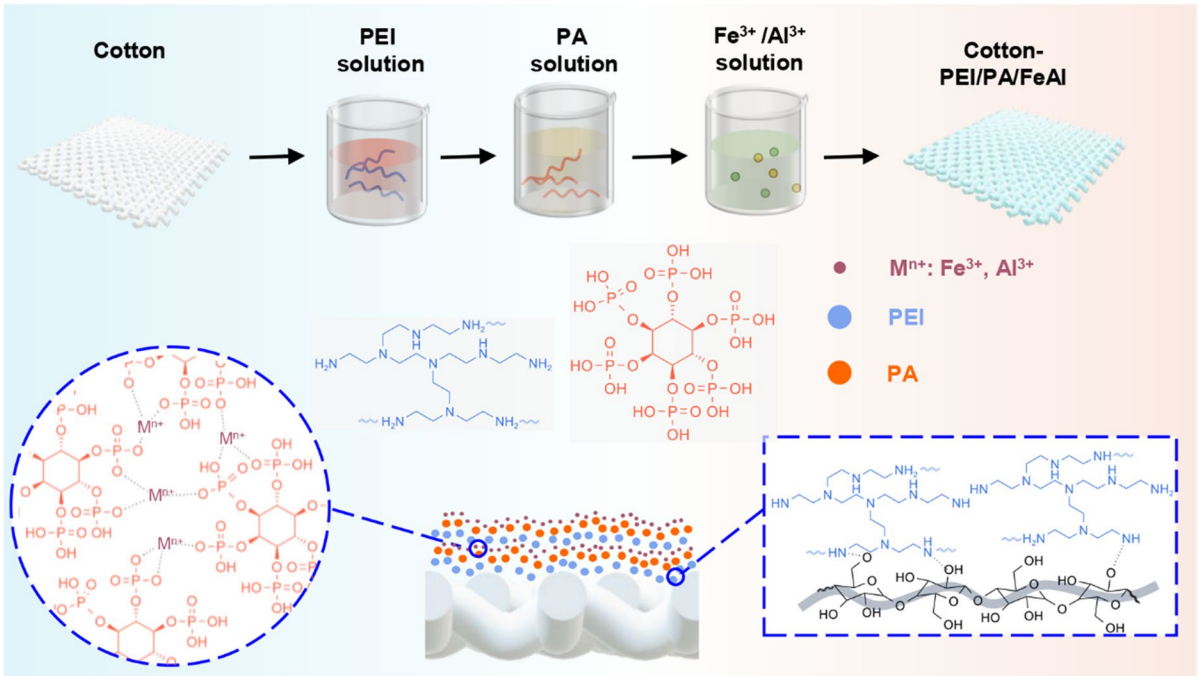

Fig. 1 Schematic diagram of preparation process of the flame-retardant and antibacterial cotton

onto the fabric because of its effect on the improved adhesion of cotton fabrics. (Chen et al. 2015) PA is sandwiched between PEI and metallic ions because of its binding effect. PA can bind well with PEI through the electrostatic interactions to form the complex IFR. In addition, PA was taken to immobilize the metallic ions through chelation by forming coordinating bonds. Noteworthily, the metallic ions were preferably deposited on the outer layer to realize their antibacterial activity and meanwhile synergizing with PEI/PA for enhanced flame-retardant property.

The functional groups on the surface of cotton fabrics can be analyzed by ATR-FTIR. As shown in Fig. 2a, the peaks in 3500 and 2895 cm^{-1} were ascribed to the stretching vibration of -OH and C-H in cellulose, respectively. After modification, these two peaks become not remarkable and quite similar to that of pure PA. This result can be explained by the location of PA on the outermost layer (to neglect the metallic ions as they do not have characteristic peaks) of cotton fabrics, which contributes to the major signals collected by FTIR. The FTIR

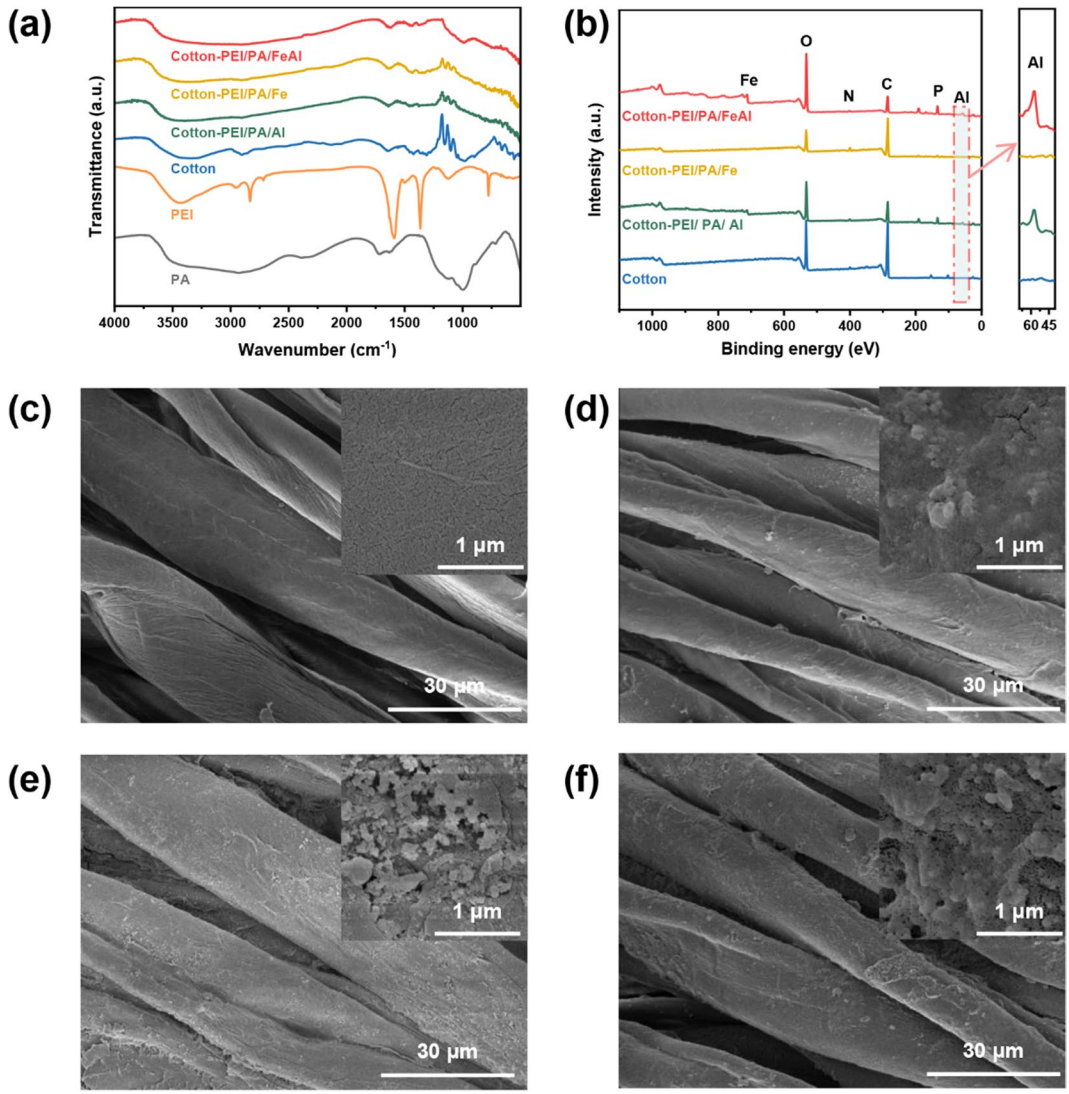

Fig. 2 Surface Structures of pure and modified cotton. **a** FTIR spectra of PA, PEI, Cotton, Cotton-PEI/PA/Al, Cotton-PEI/PA/Fe and Cotton-PEI/PA/FeAl; **b** XPS analysis of Cotton, Cotton-PEI/PA/Al, Cotton-PEI/PA/Fe and Cotton-PEI/PA/FeAl; SEM images of Cotton **c**, Cotton-PEI/PA/Al **d**, Cotton-PEI/PA/Fe **e** and Cotton-PEI/PA/FeAl **f**

spectrum of PA exhibits a sharp band centered at 989 cm^{-1} attributing to the P-O stretching vibration. The broad band at around 3500 cm^{-1} has been attributed to asymmetric OH stretching of water molecule and the weak peak at 1716 and 1625 cm^{-1} indicates H_2O deformation bending (Kim et al. 1997). While the peak in 1646 cm^{-1} was assigned to the asymmetric stretching vibration of -C=O in cellulose. The stretching vibration of C–O–C is near 977 cm^{-1}. The peaks at 3429 cm^{-1}, 2829 cm^{-1} and 1124 cm^{-1} are stretching vibration peaks of -N–H, -C-H, and -C-N while the peaks at 1580 and 1362 cm^{-1} are bending vibration peaks of -N–H and -C-H, all of which are characteristic peaks from PEI (Qi et al. 2023). The peaks observed around 1176 cm^{-1} corresponded to the stretching vibration of C-O bonds present in cellulose molecular chains. In the spectra of the coated samples, a reduction in peak intensity was noted compared to that of pure cotton, which could be attributed to the complexation of metal ions leading to a decrease in the electron density of the oxygen cloud (Zhang et al. 2021). Moreover, the peak intensity of C-O bond peaks derived from Cotton-PEI/PA/FeAl further reduced due to the enhanced complexation owning to the presence of both metal ions.

Figure 2b shows the XPS spectra with characteristic peaks of N (1 s: 401 eV), P (2p: 133 eV), Fe (2p: 711 eV), and Al (2p: 57 eV) clearly detected on the modified cotton fabrics. SEM images exhibit the surface morphologies of cotton fibers (Fig. 2c-f). After coating treatment, it is still clear to visualize individual fibers with relatively rougher substructure than the pristine fibers. This result suggests that coating components were adequately deposited on each single fiber without masking the pores among fibers. Thus, it is estimated that the physical properties of cotton fabrics, such as water vapor permeability, do not have significant differences before and after coating treatment. The related experiment will be discussed in the following section.

The surface roughness of modified cotton fibers can be interpreted by the presence of PEI, PA, and metallic ions. To evaluate whether the coating components were uniformly deposited on cotton fabrics, EDS mapping was carried out to show the distribution of key elements (Fig. 3). Exemplified by the Cotton-PEI/PA/FeAl, the C, N, O, P, Fe, and Al elements were mapped uniformly distributing on the cotton fibers, indicating an even coating treatment.

Physical properties of cotton fabrics

The dynamic change in the static water contact angle before and after coating is shown in Fig. 4a. When a droplet was placed on the pristine cotton fabric, the water contact angle was 70.0°, which decreased to 0° within 0.25 s. This was due to the abundant -OH groups on the surface of cotton fabrics, showing good hydrophilic characteristics. In addition, the capillary effect induced by the geometry of fibers

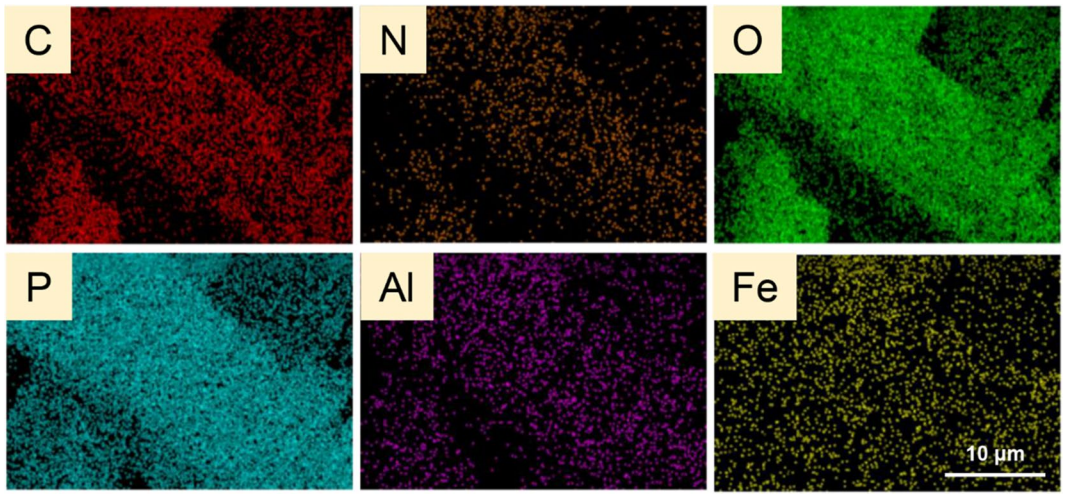

Fig. 3 EDS elemental mapping analysis of Cotton-PEI/PA/FeAl

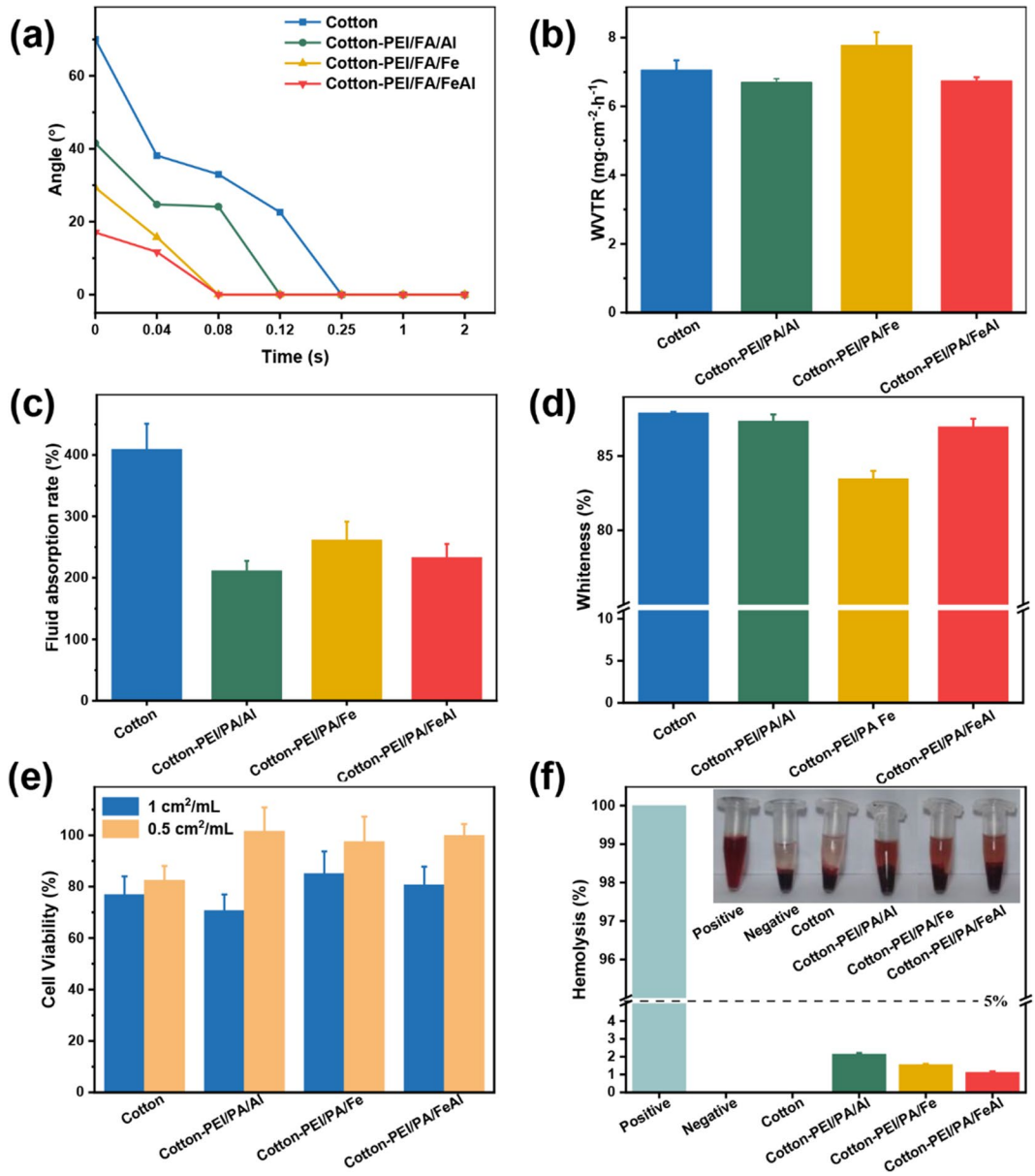

Fig. 4 Physical properties and biocompatibility of pure and modified cotton. The result of Cotton, Cotton-PEI/PA/Al, Cotton-PEI/PA/Fe, and Cotton-PEI/PA/FeAl in dynamic variation of static water contact angle **a** ; water vapor transmission rate **b** fiquid absorption rate **c**; whiteness **d**; cell viability by using L929 **e** and blood compatibility **f**

and porous fabric structure enabled rapid spreading and absorption of the water droplet. Interestingly, the initial water contact angles for all the modified cotton fabrics were decreased by 41.5° for Cotton-PEI/PA/Al, 29.4° for Cotton-PEI/PA/Fe, and 17.1° for Cotton-PEI/PA/FeAl. And it takes less time for them to decrease the water contact angle to 0° with 0.12 s recorded for Cotton-PEI/PA/Al and 0.08 s for both Cotton-PEI/PA/Fe and Cotton-PEI/PA/FeAl. The improved hydrophilicity of modified cotton fabrics can be attributed to the surface roughness of the coating layers made by the PEI and PA that contains abundant hydrophilic groups (such as -NH, NH_2 and -P-OH,) and the metallic ions. Although

the surface hydrophilicity of modified cotton fabrics was improved, their water vapor permeability is similar to pristine ones with no significant difference observed. As shown in Fig. 4b, the water vapor permeability of pristine cotton fabrics was measured at 7.04 ± 0.29 mg·cm^{-2}·h^{-1}, while it was 6.69 ± 0.11, 7.77 ± 0.39 and 6.74 ± 0.11 mg·cm^{-2}·h^{-1} for Cotton-PEI/PA/Al, Cotton-PEI/PA/Fe and Cotton-PEI/PA/FeAl, respectively. It suggests that the pore structure of cotton fabrics was not affected by the modification, which is line with the estimation based on the SEM result in Fig. 2.

As shown in Fig. 4c, the liquid absorption rate of pristine cotton fabrics was measured as $409.41 \pm 41.47\%$ because of high hydrophilicity and porous structure, allowing the water not only to spread on the fiber surface but also to be absorbed into the interior of fibers. However, the liquid absorption rate of modified cotton fabrics was largely decreased by $211.23 \pm 16.18\%$, $261.53 \pm 29.87\%$, and $233.30 \pm 21.60\%$ for Cotton-PEI/PA/Al, Cotton-PEI/PA/Fe and Cotton-PEI/PA/FeAl, respectively. Although the coating components rendered slightly improved hydrophilicity on the surface of cotton fabrics, the formed layer masked the fiber to limit the water molecules entering into the interiors of cotton fibers. The mechanical properties of the control and the flame-retardant cotton fabrics were summarized in Fig. S1 and Table S1. Notably, the warp and weft tensile stress at break of the fabrics exhibited no significant change after coating, while the breaking elongation increased compared to the that of initial cotton fabric. This observation might result from the mechanical properties of the coatings formed by PEI and PA (Zhang et al. 2021). Disparities in breaking elongation between the warp and weft directions of the fabrics could be attributed to the varying fiber densities. Importantly, the coating process preserved and did not destroy the original fiber and weaving structure, in contrast, the overall mechanical properties were enhanced which will be beneficial to the practical use.

The effect of modification on the cotton whiteness was evaluated in Fig. 4d. It is interesting to find that the aluminum ions can retain the cotton whiteness, evidenced by the Cotton-PEI/PA/Al and Cotton-PEI/PA/FeAl having the whiteness value of $87.35 \pm 0.44\%$ and $86.96 \pm 0.54\%$, comparable to that of pristine cotton fabrics ($87.89 \pm 0.07\%$). It is worth noting that iron ions induced yellowish color to the cotton fabrics, leading to the reduced whiteness of $83.47 \pm 0.52\%$ as measured on Cotton-PEI/PA/Fe. Nevertheless, the adverse effect caused by iron ions can be eliminated by the addition of aluminum ions.

The biocompatibility of multifunctional cotton fabrics was evaluated by the cell viability and hemolysis. As shown in Fig. 4e, the cell viability for cotton fabrics before or after treatment was all higher than 70%, indicating good biocompatibility of testing samples according to the standard. In comparison with pristine cotton fabrics, the cell viability of modified cotton fabrics was higher, especially in the concentration of 1 cm^2/mL. After coating treatment, the surface hydrophilicity was improved with better adhesion for the cell proliferation. This result is in good agreement with that in Fig. 4a. Pristine cotton fabrics show excellent blood compatibility (Fig. 4f) and even after modification all the samples exhibit the hemolysis rate below 5%, which was considered acceptable blood compatibility according to the ASTM F756-00 Non-Contact Biological Materials Standard (Weber et al. 2018). In other words, the coating treatment had minimal impact on the blood compatibility of cotton fabrics, making them promising candidate for healthcare and medical applications.

Antibacterial performance

As metallic ions, i.e. Al^{3+} and Fe^{3+}, were deposited on the surface of cotton fabrics, their effect on the improvement of antibacterial performance was evaluated according to GB/T 20944.2–2007. As shown in Fig. 5a, more bacterial colonies were observed on the agar plates for the pristine cotton fabric than the control, which was attributed to the porous structure of cotton fabrics providing abundant sites for bacterial colonization and growth. After coating treatment, the antibacterial activities were largely enhanced for all three samples doped with Al^{3+} and/or Fe^{3+}, presenting the best result when both metallic ions were combined (Luo et al. 2021; Gong et al. 2022). Cotton-PEI/PA/Al samples showed 88.5% and 71.3% bactericidal efficacy against *S. aureus* and *E. coli.* Cotton-PEI/PA/Fe samples showed 99.2% and 94.3% bactericidal efficacy against *S. aureus* and *E. coli*. There was no bacterial growth after the bacterial solution coated plate was in contact with PEI/PA/FeAl-coated treated cotton fabrics,

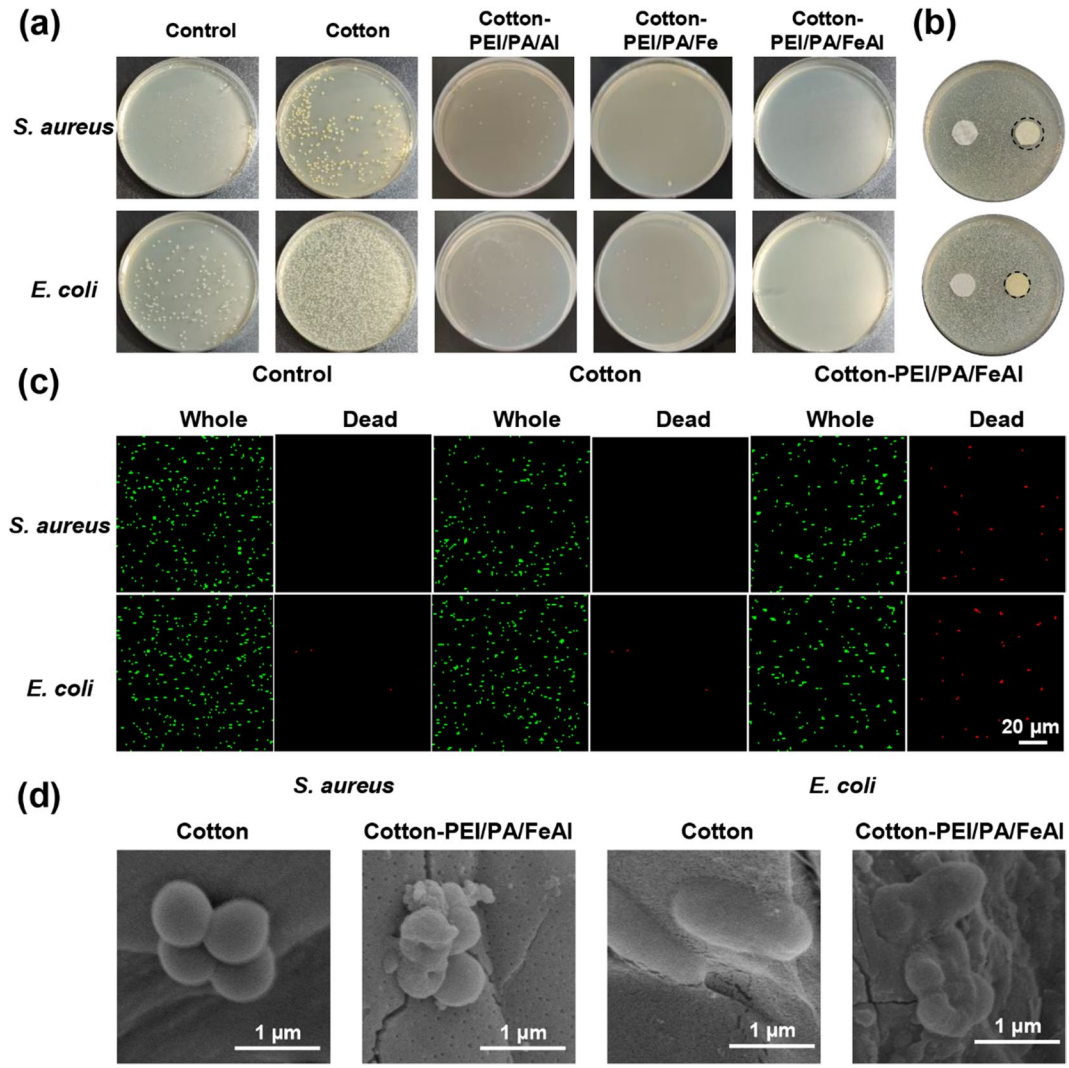

Fig. 5 Antibacterial performance of pure and modified cotton fabrics. **a** Comparison of antibacterial activity for Cotton, Cotton-PEI/PA/Al, Cotton-PEI/PA/Fe, and Cotton-PEI/PA/FeAl; **b** Zone of inhibition for Cotton (left) and Cotton-PEI/PA/FeAl (right); **c** Bacteria stained to show the live and dead cells; **d** SEM images to show the morphology of *S. aureus* and *E. coli* for Cotton and Cotton-PEI/ PA/FeAl

and the bactericidal efficacy was more than 99.9% for both bacteria. The MIC values of the metal ions and the FIC values of both metal ions were further validated as shown in Table S2. For *S. aureus*, the MIC of $Fe_2(SO_4)_3$ was 18.5 μg/mL, and for *E. coli*, it was 18.0 μg/mL. Similarly, the MICs of $Al_2(SO_4)_3$ were 18.5 μg/mL for *S. aureus* and 18.0 μg/mL for *E. coli*. The calculated FIC was 0.84 for *S. aureus* and 0.92 for *E. coli*, indicating an additive antibacterial effect of the two metal ions.

In Fig. 5b, zone of inhibition was examined to compare the antibacterial property before and after coating treatment. As expected, no antibacterial rings around the pristine cotton fabric, and colonies grew densely at the fabric edge. Distinctly, Cotton-PEI/PA/FeAl exhibited an antibacterial ring diameter of 1.9 cm and a bandwidth of 2 mm against *S. aureus* and 1.7 cm and 1 mm against *E. coli*. According to the evaluation standard GB/T 20944.1–2007, Cotton-PEI/ PA/FeAl demonstrated good antibacterial

effects. As shown in Fig. 5c, further assessment of the antibacterial performance was conducted using Live/Dead dual-color fluorescent dyes, where Syto 9 and PI were used as green and red dyes to stain the live and dead bacteria, respectively. When compared with the control and pristine cotton fabrics, largely improved antibacterial performance was determined on Cotton-PEI/ PA/FeAl with less green but more red fluorescence imaged by CLSM. The structure and morphology of bacteria can be well observed by SEM

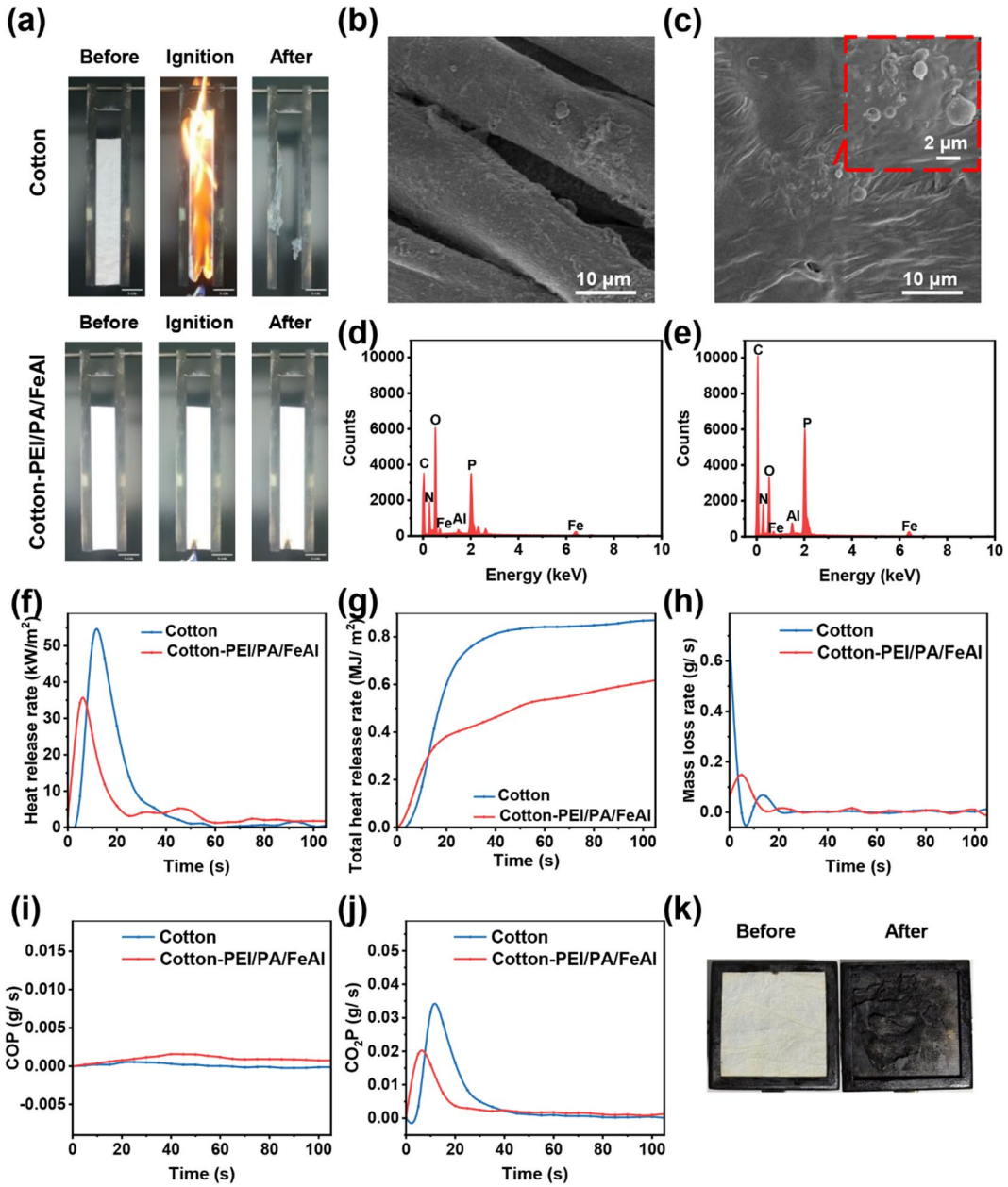

Fig. 6 Vertical combustion images **a** of Cotton, Cotton-PEI/ PA/FeAl; SEM images of Cotton-PEI/PA/FeAl before **b** and after **c** the vertical combustion; EDS result of Cotton-PEI/PA/ FeAl before **d** and after **e** the vertical combustion; The curves of heat release rate **f**, total heat release **g**, mass loss rate **h**, CO production **i**, and CO_2 production **j** of Cotton, Cotton-PEI/PA/ FeAl in the CCT test; Photographs **k** of cotton-PEI/PA/FeAl before and after cone calorimetry testing

(Fig. 5d). For pristine cotton fabrics, no antibacterial performance was found to allow the *E. coli* and *S. aureus* retain the original rod-shaped and spherical structures. However, in contact with antibacterial cotton fabrics, the bacteria showed the signs of death cells with remarkable morphological changes, collapsed structures, and even leaked intracellular substances. Taken together, these results demonstrate good antibacterial efficacy on the Al^{3+}/Fe^{3+}-incorporated cotton fabrics.

Flame retardant properties

The flame retardancy of the Cotton-PEI/PA/Al is evaluated under an open fire, high-temperature and strong heat flux conditions, respectively. Vertical burning experiments and LOI tests were conducted to evaluate the performance of test samples under open flame. As shown in Fig. 6a and SI Video1-2, the pristine cotton fabric was immediately ignited, continued to burn for 17 s after the flame was removed, exhibited non-flaming combustion for 23 s, and produced a small amount of char residue, with a LOI of 18.0%. The modified cotton fabric showed resistance toward ignition, and after the flame was removed it exhibited glowing combustion for 1 s before extinguishing, leaving a 2.5-cm long carbon mark while preserving the integrity of the fabric, with a LOI of 35.0%. The LOI of Cotton-PEI/PA/Al and Cotton-PEI/PA/Fe were 32.5% and 28.5%, respectively, indicating that two metallic ions had a synergistic effect on the flame retardance of the fabric.

The morphology and surface element distribution of Cotton-PEI/PA/FeAl before and after vertical combustion was observed using SEM (Fig. 6b-c) and EDS (Fig. 6d-e). The fiber morphology was clearly observed on the Cotton-PEI/PA/FeAl, however after combustion, the char residues were formed by the IFR system to cover the surface of the fabric and protect it from further burning. The globular particles were also observed because of the trapped gas bubbles released from the IFR. The relative elemental content of C, P, Fe, and Al on the surface of the char layer after combustion was higher than before combustion, whereas the content of N and O elements were lower, indicating the outgassing of N and O as gaseous species to form the carbon–nitrogen-phosphorus-containing char residues.

Table 1 Key data from CCT tests

	Cotton	Cotton-PEI/PA/FeAl
TTI (s)	7	8
PHRR (kW/m^2)	50.67	25.41
$T_{pk\text{-}HRR}$ (s)	10	10
THR (MJ/m^2)	0.87	0.62
TSP (m^2)	0.1	0.1
Mean-EHC (MJ/Kg)	4.37	6.20
CO (Kg/Kg)	0.002	0.182
CO_2 (Kg/Kg)	0.436	0.306

TTI: Time to Ignition; PHRR: Peak of Heat Release Rate; tpk-HRR: Time to Peak Heat Release Rate; TSP: Total smoke production; Mean-EHC: Mean value of Effective Heat of Combustion

Additionally, the combustion behavior of pristine cotton fabrics and Cotton-PEI/PA/FeAl under high heat flux density was studied using the Cone Calorimetry Test (CCT). The curves for Heat Release Rate (HRR), Total Heat Release Rate (THRR), Mass Loss Rate (MLR), Carbon Monoxide Production (COP), and Carbon Dioxide Production (CO_2P) are shown in Fig. 6g-j with key parameters summarized in Table 1. Cotton-PEI/PA/FeAl underwent complete thermal decomposition with a Peak Heat Release Rate (PHRR) of 50.67 kW/m^2, which was about two times higher than that (25.41 kW/m^2) of pristine cotton fabrics that did not completely decompose. The unit mass of the coated fabric generated more CO and less CO_2 compared to the uncoated fabric due to the production of more non-combustible gases (H_2O and NH_3) during the decomposition process, CO cannot come into full contact with O_2, resulting in incomplete CO combustion. The Total Smoke Production (TSP) remained constant before and after coating,

Fig. 7 TGA curves **a** and DTG curves **b** of Cotton, Cotton-PEI/PA/Fe, Cotton-PEI/PA/Al, Cotton-PEI/PA/FeAl in air atmosphere; TGA curves **c** and DTG curves **d** of Cotton, Cotton-PEI/PA/Fe, Cotton-PEI/PA/Al, Cotton-PEI/PA/FeAl in nitrogen atmosphere; 3D TG-IR spectra of Cotton **e**, Cotton-PEI/PA/FeAl fabrics **f**; FTIR spectra **g** of decomposition products at the maximum rate of thermal decomposition of Cotton (at 502.02 s) and Cotton-PEI/PA/FeAl (at 391.00 s), FTIR spectra of products at the late stage of thermal decomposition of Cotton-PEI/PA/FeAl (at 568.90 s); Schematic illustration **h** of the possible flame-retardant mechanism ▶

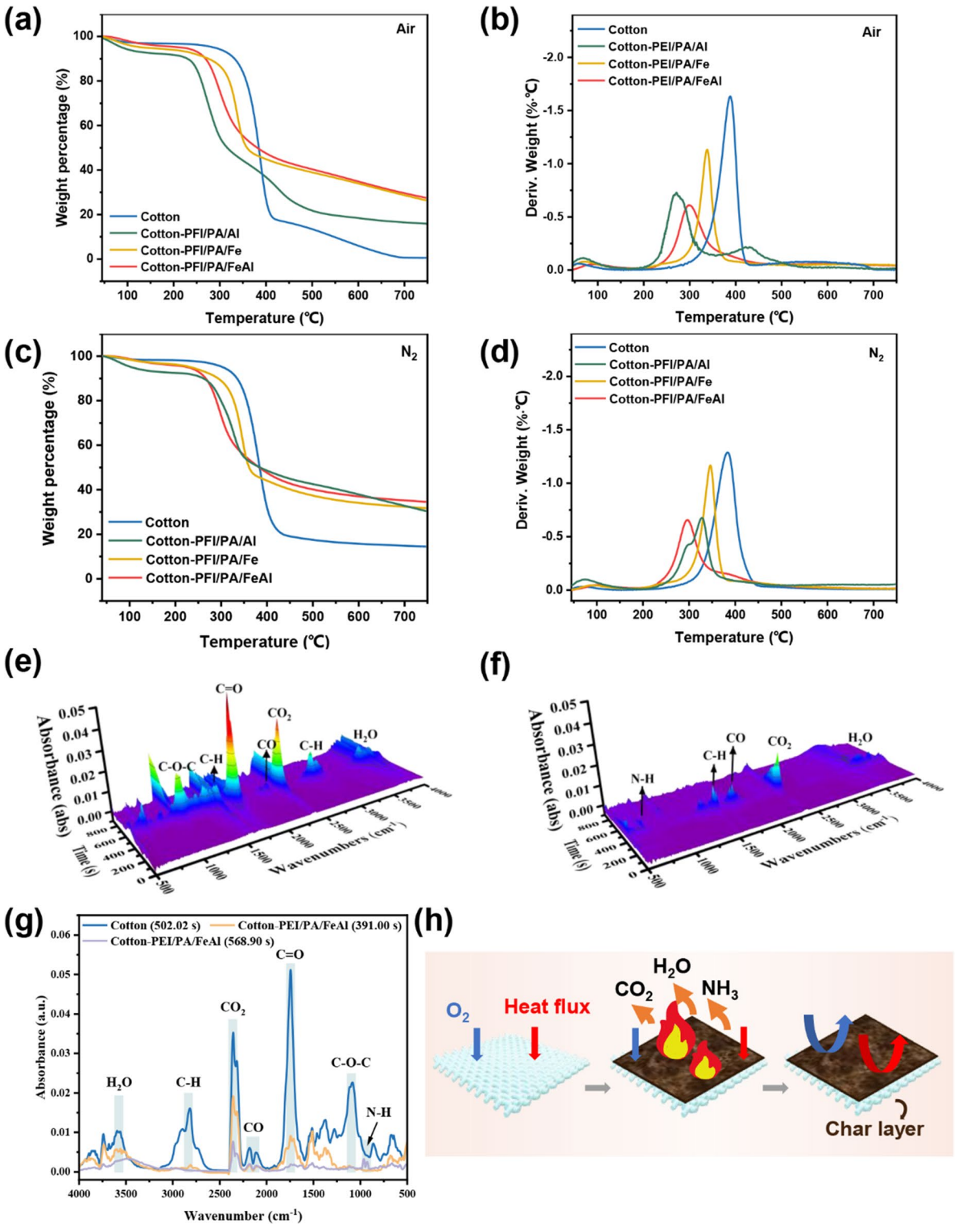
(a)
Air
Weight percentage (%)
Temperature (℃)
Cotton
Cotton-PFI/PA/Al
Cotton-PFI/PA/Fe
Cotton-PFI/PA/FeAl
(b)
Air
Deriv. Weight (%/℃)
Temperature (℃)
Cotton
Cotton-PEI/PA/Al
Cotton-PEI/PA/Fe
Cotton-PEI/PA/FeAl
(c)
N2
Weight percentage (%)
Temperature (℃)
(d)
N2
Deriv. Weight (%/℃)
Temperature (℃)
(e)
Absorbance (abs)
Time (s)
Wavenumbers (cm-1)
C=O
CO2
C-O-C
C-H
CO
C-H
H2O
(f)
Absorbance (abs)
Time (s)
Wavenumbers (cm-1)
N-H
C-H
CO
CO2
H2O
(g)
Cotton (502.02 s)
Cotton-PEI/PA/FeAl (391.00 s)
Cotton-PEI/PA/FeAl (568.90 s)
Absorbance (a.u.)
Wavenumber (cm-1)
H2O
C-H
CO2
C=O
CO
C-O-C
N-H
(h)
O2
Heat flux
H2O
CO2
NH3
Char layer

indicating that the coating released less smoke during combustion. In comparison with the pristine cotton fabrics, more CO and less CO_2 were detected on the modified fabrics, which was in good agreement with the results in Fig. 6i-j. Further, the durability and washing resistance of the coating were investigated in terms of UV radiation, water washing, and soaping. The results, presented in Fig. S2 and Table S3-5, indicated that the coated fabrics maintained good flame retardancy properties with a LOI of 35.0% after 7 days of UV radiation. The LOI of the coated fabric decreased from 35.0% to 32.5% after undergoing 30 cycles of pure water washing. Moreover, after 20 cycles of soaping, the LOI decreased from 35.0% to 28.3%, indicating a significant decline in flame retardancy. This phenomenon can be attributed to the fact that the surfactants in the detergent reduce the surface tension of the water, which facilitates better penetration of the water into the fibers and coatings, resulting in the detachment of coatings from the fiber surface.

The thermal stability of cotton fabrics was evaluated through thermogravimetric analysis (TGA). Figure 7a-d depicts the TGA and DTG curves for the pristine and modified cotton fabrics with corresponding data listed in Table 1. As shown in Fig. 7a-b, in air atmosphere, the pristine cotton fabric exhibited two decomposition stages: the first stage (with a mass loss rate of approximately 84%) occurred between 287 °C and 437 °C, where long-chain cellulose was degraded to generate glucose and further decomposed into smaller molecules; the second stage occurred between 450 °C and 680 °C, where the small molecules generated in the previous stage underwent further oxidation (Liu et al. 2018). As detailed in Table 2 and Fig. 7, the residual carbon content of pristine cotton fabrics at 750 °C was only 0.50% with the highest decomposition rate at 383.7 °C (T_{max}). After modification, the residual carbon content at 750 °C was sharply improved to 15.8 wt%, 26.4 wt%, and 27.5 wt% respectively for Cotton-PEI/PA/Al, Cotton-PEI/PA/Fe, and Cotton-PEI/PA/FeAl. It seems that the iron ion was more effective than aluminum ion in the improvement of residual carbon content. Noteworthily, $T_{5\%}$ and T_{max} were decreased after modification treatment on cotton fabrics. The reason behind this is that the PEI/PA/metallic ions in IFR system altered the thermal decomposition process of the cotton fabric to induce the dehydration, condensation, and cross-linking that occurred at lower temperatures, resulting in a denser carbon layer on the fabric surface to help reduce the rate of flammable gas production and fabric decomposition. As earlier reported, PA decomposes at lower temperatures, producing phosphoric acid and polyphosphoric acid, accelerating cellulose dehydration and carbonization, thereby forming a carbon layer barrier prematurely, impeding the transfer of heat and flammable gas, and protecting the material from further degradation (Shi et al. 2018). As shown in Fig. 7c-d, in N_2 atmosphere, the residual carbon content of the pristine cotton fabric at 750 °C was increased to 14.5%, significantly higher than that in air atmosphere. However, this value was still less than 50% of that on modified cotton fabrics, which demonstrate improvement on the thermal stability both in Air and N_2 atmosphere. In the case of N_2 atmosphere, the synergy of aluminum and iron ions was observed on the residual carbon content at 750 °C. The $T_{5\%}$ and T_{max} under N_2 atmosphere reflected the decomposition behaviors similar to air atmosphere. The improvement on thermal stability with higher residual carbon content at 750 °C indicate the enhanced flame retardance of modified cotton fabrics.

To elucidate the degradation mechanism of the fabric, TG-IR was utilized to detect the gas products after thermal degradation. From the 3D TG-IR spectra (Fig. 7e-g), it can be observed that the coated fabric exhibited lower absorbance of volatile products and reached the release peak earlier compared to the uncoated fabric. Volatile product functional groups exhibited similar absorption peak positions around

Table 2 Summary of key data from TGA and DTA in air and nitrogen atmosphere

Sample	$T_{5\%}$ (℃)		T_{max1} (℃)		$T_{75\%}$ (℃)		Residue at 750 ℃ (wt%)	
	N_2	Air	N_2	Air	N_2	Air	N_2	Air
Cotton	303.9	288.4	385.5	383.7	412.1	401.9	14.5	0.50
Cotton-PEI/PA/Al	105.2	99.4	327.4	282.2	/	/	30.4	15.8
Cotton-PEI/PA/Fe	234.4	136.9	346.2	338.9	/	/	31.7	26.4
Cotton-PEI/PA/FeAl	227.9	217.9	295.3	293.8	/	/	34.5	27.5

3654 cm^{-1} (-OH), 2810 cm^{-1} (C-H hydrocarbons), 2358 cm^{-1} (CO_2), 1743 cm^{-1} (C = O), and 1093 cm^{-1} (C–O–C), as shown in the Fig. 7g. Thanks to the IFR, the char residues covered on the cotton fabrics will protect them from burning, which could be well evidenced by comparing the absorption of C = O and C–O–C that were the characteristic groups in cotton. These absorption peaks mainly belong to the gaseous products of cellulose pyrolysis. The content of volatile products (hydrocarbons, carbonyl compounds, and ether compounds) in the modified cotton fabric was significantly lower than that of the control group, indicating that the modified cotton fabric tended to char at high temperatures, leading to a reduction in volatile products. A peak for N–H appeared at 9967 cm^{-1} in the modified fabric, indicating that the nitrogen-containing PEI generated non-combustible gas (NH_3), which help diluting combustible gases. No peaks related to P elements were detected in the gas phase, indicating that PA primarily functioned in the condensed phase. Compared to the pristine cotton fabric, the absorbance of flammable gas products (CO, C-O, C–O–C) of the coated fabric decreased, reducing the flammability gas products which could slow down the flame spread on the fabric.

Based on these results, a possible flame-retardant mechanism was proposed (Fig. 7h). At the time of combustion, the flame-retardant coatings can prevent cotton fabrics from burning via the synergy of phosphorus-nitrogen intumescent flame-retardant system. In detail, PA degrades during combustion and catalyzes the dehydration and carbonization of cellulose, forming a carbon barrier that impedes heat flow and the transfer of combustible gases. Meanwhile, PEI with high nitrogen content decomposes into nonflammable volatiles to dilute the combustible gas and further inhibits the combustion process.

Conclusion

In summary, through layer-by-layer assembly, the cotton fabric was functionalized using PEI/PA/FeAl system to obtain good biocompatibility, antibacterial and flame-retardant properties. In comparison with the pristine cotton fabric, no significant difference was observed on the modified one in terms of WVTR and whiteness. Whereas the fluid absorption rate was reduced after coating treatment. Interestingly, the modified cotton fabric demonstrated excellent cell viability and blood compatibility. Regarding antibacterial property, Fe^{3+} and Al^{3+} that were deposited on the most outer layer of cotton fabrics served as the main component to show the synergistic effect with 99.2% and 94.3% bactericidal efficacy against *S. aureus* and *E. coli*, respectively. Thanks to the PEI/PA/FeAl system, the modified cotton fabric showed remarkable flame-retardant property in the vertical burning experiment with a LOI of 35%. Further supported by the CCT, TGA and TG-IR, the underlying flame-retardant mechanism of Cotton-PEI/PA/FeAl was elucidated to show that the char layer was rapidly induced to form by the thermal decomposition of PEI/PA and facilitated by the metallic ions, ultimately protecting the cotton fabric from burning.

Acknowledgements This work is financially sponsored by the National Natural Science Foundation of China (No. 52073186), Funding for Distinguished Young Scholars of Sichuan Province (23NSFJQ0001), Strategic Cooperation Projects of Yi Bin City and Sichuan University (No. 2020CDYB-6), Sichuan University Postdoctoral Interdisciplinary Innovation Fund (No. JXCK2231) and Funding of Engineering Characteristic Team, Sichuan University (2020SCUNG122).

Author contributions Qingyi Li, Yakun Zong: Methodology, Experiment, Writing-Original draft preparation, Revision; Yuanzhang Jiang: Investigation, Software; Ruifang Zhao: Resources; Jun Zhang, Yidong Shi: Methodology, Investigation; Jianming Chen, Lin TAN: Conceptualization, Writing-Review & Editing, Supervision, Revision.

Funding This work is financially sponsored by the National Natural Science Foundation of China (No. 52073186), Funding for Distinguished Young Scholars of Sichuan Province (23NSFJQ0001), Strategic Cooperation Projects of Yi Bin City and Sichuan University (No. 2020CDYB-6), Sichuan University Postdoctoral Interdisciplinary Innovation Fund (No. JXCK2231) and Funding of Engineering Characteristic Team, Sichuan University (2020SCUNG122).

Declarations

Competing interests The authors declare no competing interests.

Consent for publication All authors have given approval to the final version of the manuscript.

Ethical approval All the authors state that they adhere to the Ethical Responsibilities of Authors. In addition, this article does not contain any studies with human participants or animals performed by any of the authors.

Competing Interests The authors declare no competing interests.

References

Barbalini M, Bartoli M, Tagliaferro A, Malucelli G (2020) Phytic Acid and Biochar: An Effective All Bio-Sourced Flame Retardant Formulation for Cotton Fabrics. Polymers 12:811. https://doi.org/10.3390/polym12040811

Chen S, Li X, Li Y, Sun J (2015) Intumescent Flame-Retardant and Self-Healing Superhydrophobic Coatings on Cotton Fabric. ACS Nano 9:4070–4076. https://doi.org/10.1021/acsnano.5b00121

Chen S, Li H, Lai X et al (2021) Superhydrophobic and phosphorus-nitrogen flame-retardant cotton fabric. Prog Org Coat 159:106446. https://doi.org/10.1016/j.porgcoat.2021.106446

Cheng X-W, Tang R-C, Yao F, Yang X-H (2019) Flame retardant coating of wool fabric with phytic acid/polyethyleneimine polyelectrolyte complex. Prog Org Coat 132:336–342. https://doi.org/10.1016/j.porgcoat.2019.04.018

Ding D, Liu K, Liu Y et al (2023) A durable formaldehyde-free flame retardant containing phosphamide and ammonium phosphate for cotton fabrics. Cellulose 30:11195–11209. https://doi.org/10.1007/s10570-023-05540-x

Fang F, Ran S, Fang Z et al (2019) Improved flame resistance and thermo-mechanical properties of epoxy resin nanocomposites from functionalized graphene oxide via self-assembly in water. Compos B Eng 165:406–416. https://doi.org/10.1016/j.compositesb.2019.01.086

Fang F, Huo S, Shen H et al (2020) A bio-based ionic complex with different oxidation states of phosphorus for reducing flammability and smoke release of epoxy resins. Composites Communications 17:104–108. https://doi.org/10.1016/j.coco.2019.11.011

Gong D, Zhang A, Luo H et al (2022) Polyhexamethylene biguanide hydrochloride anchored polymeric elastic fibers with robust antibacterial performance. J of Applied Polymer Sci 139:51633. https://doi.org/10.1002/app.51633

Hao S, Zhu W, Huang H et al (2019) A Phosphorous-Aluminium-Nitride Synergistic Flame Retardant to Enhance Durability and Flame Retardancy of Cotton. ChemistrySelect 4:13952–13958. https://doi.org/10.1002/slct.201903370

Hemaiswarya S, Kruthiventi AK, Doble M (2008) Synergism between natural products and antibiotics against infectious diseases. Phytomedicine 15:639–652. https://doi.org/10.1016/j.phymed.2008.06.008

Holder KM, Smith RJ, Grunlan JC (2017) A review of flame retardant nanocoatings prepared using layer-by-layer assembly of polyelectrolytes. J Mater Sci 52:12923–12959. https://doi.org/10.1007/s10853-017-1390-1

Horrocks AR (2011) Flame retardant challenges for textiles and fibres: New chemistry versus innovatory solutions. Polym Degrad Stab 96:377–392. https://doi.org/10.1016/j.polymdegradstab.2010.03.036

Kappes RS, Urbainczyk T, Artz U et al (2016) Flame retardants based on amino silanes and phenylphosphonic acid. Polym Degrad Stab 129:168–179. https://doi.org/10.1016/j.polymdegradstab.2016.04.012

Kim H-N, Keller SW, Mallouk TE et al (1997) Characterization of Zirconium Phosphate/Polycation Thin Films Grown by Sequential Adsorption Reactions. Chem Mater 9:1414–1421. https://doi.org/10.1021/cm970027q

Lambert E, Aguié-Béghin V, Dessaint D et al (2019) Real Time and Quantitative Imaging of Lignocellulosic Films Hydrolysis by Atomic Force Microscopy Reveals Lignin Recalcitrance at Nanoscale. Biomacromol 20:515–527. https://doi.org/10.1021/acs.biomac.8b01539

Lazar ST, Kolibaba TJ, Grunlan JC (2020) Flame-Retardant Surface Treatments Nat Rev Mater 5:259–275. https://doi.org/10.1038/s41578-019-0164-6

Li N, Han H, Li M et al (2021) Eco-friendly and intrinsic nanogels for durable flame retardant and antibacterial properties. Chem Eng J 415:129008. https://doi.org/10.1016/j.cej.2021.129008

Li Y, Sun L, Wang H et al (2023) A novel composite coating containing P/N/B and bio-based compounds for flame retardant modification of polyester/cotton blend fabrics. Colloids Surf, A 660:130826. https://doi.org/10.1016/j.colsurfa.2022.130826

Liu L, Huang Z, Pan Y et al (2018) Finishing of cotton fabrics by multi-layered coatings to improve their flame retardancy and water repellency. Cellulose 25:4791–4803. https://doi.org/10.1007/s10570-018-1866-4

Liu G, Bao Z, Wu J (2020) Injectable baicalin/F127 hydrogel with antioxidant activity for enhanced wound healing. Chin Chem Lett 31:1817–1821. https://doi.org/10.1016/j.cclet.2020.03.005

Luo H, Yin X-Q, Tan P-F et al (2021) 2021 Polymeric antibacterial materials: design, platforms and applications. J Mater Chem B 9:2802–2815. https://doi.org/10.1039/D1TB00109D

Osimitz TG, Kacew S, Hayes AW (2019) Assess flame retardants with care. Science 365:992–993. https://doi.org/10.1126/science.aay6309

Özer MS, Gaan S (2022) Recent developments in phosphorus based flame retardant coatings for textiles: Synthesis, applications and performance. Prog Org Coat 171:107027. https://doi.org/10.1016/j.porgcoat.2022.107027

Page J, Whaley P, Bellingham M et al (2023) A new consensus on reconciling fire safety with environmental & health impacts of chemical flame retardants. Environ Int 173:107782. https://doi.org/10.1016/j.envint.2023.107782

Qi P, Li Y, Yao Y et al (2023) 2023 Ultra washing durable flame retardant coating for cotton fabric by the covalent bonding and interface polymerization. Chem Eng J 452:139453. https://doi.org/10.1016/j.cej.2022.139453

Rao W, Shi J, Yu C et al (2021) Highly efficient, transparent, and environment-friendly flame-retardant coating for cotton fabric. Chem Eng J 424:130556. https://doi.org/10.1016/j.cej.2021.130556

Shi X-H, Chen L, Liu B-W et al (2018) Carbon Fibers Decorated by Polyelectrolyte Complexes Toward Their Epoxy Resin Composites with High Fire Safety. Chin J Polym Sci 36:1375–1384. https://doi.org/10.1007/s10118-018-2164-1

Sun L, Xie Y, Wu J et al (2021) A novel P/N-based flame retardant synthesized by one-step method toward cotton materials and its flame-retardant mechanism. Cellulose 28:3249–3264. https://doi.org/10.1007/s10570-021-03728-7

Sykam K, Försth M, Sas G et al (2021) Phytic acid: A bio-based flame retardant for cotton and wool fabrics. Ind Crops Prod 164:113349. https://doi.org/10.1016/j.indcrop.2021.113349

Weber M, Steinle H, Golombek S et al (2018) Blood-contacting biomaterials: in vitro evaluation of the hemocompatibility. Front Bioeng Biotechnol 6:99. https://doi.org/10.3389/fbioe.2018.00099

Wu H, Zhang R, Hu B et al (2021) A porous hydrogel scaffold mimicking the extracellular matrix with swim bladder derived collagen for renal tissue regeneration. Chin Chem Lett 32:3940–3947. https://doi.org/10.1016/j.cclet.2021.04.043

Xu F, Zhong L, Xu Y et al (2019) Highly efficient flame-retardant and soft cotton fabric prepared by a novel reactive flame retardant. Cellulose 26:4225–4240. https://doi.org/10.1007/s10570-019-02374-4

Yang CQ, Wu W, Xu Y (2005) The combination of a hydroxy-functional organophosphorus oligomer and melamine-formaldehyde as a flame retarding finishing system for cotton. Fire Mater 29:109–120. https://doi.org/10.1002/fam.877

Ye G, Huo S, Wang C et al (2021) A novel hyperbranched phosphorus-boron polymer for transparent, flame-retardant, smoke-suppressive, robust yet tough epoxy resins. Compos B Eng 227:109395. https://doi.org/10.1016/j.compositesb.2021.109395

Zhang A-N, Zhao H-B, Cheng J-B et al (2021) 2021 Construction of durable eco-friendly biomass-based flame-retardant coating for cotton fabrics. Chem Eng J 410:128361. https://doi.org/10.1016/j.cej.2020.128361